

Contribution from the Department of Chemistry,
Georgia Institute of Technology, Atlanta, Georgia 30332

A New and Convenient Method for the Preparation of Complex Metal Hydrides of Group II Metals. Synthesis of Complex Metal Hydrides of Zinc

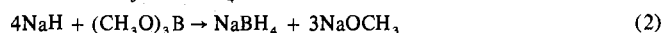
E. C. ASHBY* and JOHN J. WATKINS

Received April 16, 1973

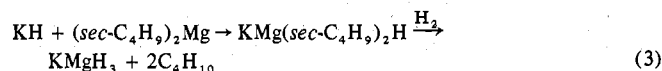
A series of complex metal hydrides of zinc with composition $M_nZn_mH_{2m+n}$, where $M = \text{Li, Na, or K}$, has been synthesized by reacting an appropriate "ate" complex of zinc ($M_nZn_mR_{2m+n}$) with either LiAlH_4 , NaAlH_4 , or AlH_3 . The 1:1, 2:1, and 3:1 complexes of methyl lithium and dimethyl zinc yielded LiZnH_3 , Li_2ZnH_4 , and Li_3ZnH_5 when allowed to react with lithium aluminum hydride in diethyl ether. The reaction of potassium hydride with dimethyl zinc in 1:1 and 1:2 ratios in tetrahydrofuran yielded potassium dimethylhydrido zincate [$\text{KZn}(\text{CH}_3)_2\text{H}$] and potassium tetramethylhydrido zincate [$\text{KZn}_2(\text{CH}_3)_4\text{H}$]. KZn_2H_5 resulted when either $\text{KZn}(\text{CH}_3)_2\text{H}$ or $\text{KZn}_2(\text{CH}_3)_4\text{H}$ was allowed to react with AlH_3 in tetrahydrofuran; whereas, KZnH_3 was obtained from the reaction of $\text{KZn}(\text{CH}_3)_2\text{H}$ with lithium aluminum hydride in the same solvent. Both the 1:1 and 1:2 complexes of sodium hydride with dimethyl zinc gave NaZnH_3 when allowed to react with sodium aluminum hydride in tetrahydrofuran. These reactions are presented as examples of a new and general route for the preparation of complex metal hydrides by the reaction of "ate" complexes with complex metal hydrides of aluminum or AlH_3 .

Introduction

Complex metal hydrides of aluminum and boron (e.g., LiAlH_4 and NaBH_4) have proven to be invaluable reagents in organic synthesis. These compounds are prepared by the reaction of a group IA metal hydride with a group IIIA metal derivative (eq 1 and 2).^{1,2} Recently we reported the prep-



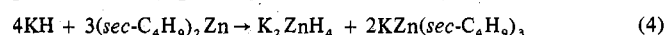
paration of the first complex metal hydride of magnesium (KMgH_3) by the hydrogenolysis of an "ate" complex of magnesium (eq 3).³ The necessity for this synthetic scheme



is due to the fact that the reaction of KH directly with MgCl_2 (analogous to the preparation of LiAlH_4) produces MgH_2 and not KMgH_3 .⁴ The particular R_2Mg compound used [$(\text{sec-Bu})_2\text{Mg}$] is difficult to prepare but its use is necessitated by the fact that it is the only known R_2Mg compound soluble in benzene and benzene solvent is necessitated due to the fact that MMgR_2H compounds (where $M = \text{Li, Na, or K}$) cleave ether solvents.^{5,6} In addition, it is known that R-Mg compounds can be hydrogenolyzed to H-Mg com-

pounds most easily when the R group is branched in the α position, such as in *sec*-butyl compounds.⁷

Analogous to the reaction of KH with MgCl_2 , the reaction of KH with ZnCl_2 , NaH with ZnI_2 , or LiH with ZnBr_2 all yield ZnH_2 instead of complex metal hydrides of zinc. For this reason the synthesis of K_2ZnH_4 and Na_2ZnH_4 ,⁸ reported recently, was carried out by reaction of an "ate" complex of zinc (eq 4). In view of this success we wished to



expand our synthetic studies to include other complex metal hydrides of zinc. Our initial plan was to investigate the reaction of LiH with di-*sec*-butylzinc in both hydrocarbon and ether solvents in an attempt to prepare a spectrum of lithium dialkylzinc hydrides ranging from $\text{Li}_3\text{ZnR}_2\text{H}_3$ to $\text{LiZn}_3\text{R}_6\text{H}$, where $R = \text{sec-butyl}$. The lithium dialkylzinc hydrides were to be converted to the corresponding complex metal hydrides by high-pressure hydrogenation, since the carbon-zinc bond of the *sec*-butylzinc group should be easily converted to an H-Zn bond by hydrogenation (see eq 3).

Our initial plan proved to be unfeasible when the intermediate lithium *sec*-butylzinc hydrides were found to cleave ether solvents too rapidly for hydrogenation to be an effective tool for R-Zn to H-Zn conversion. Unfortunately, the above reaction did not take place at all in benzene. The plan was modified in two ways. First, conversion of R-Zn to H-Zn was carried out by reaction of the "ate" complex with LiAlH_4 since alkyl exchange from zinc to aluminum and hydrogen exchange from aluminum to zinc might be expected at temperatures lower than 0° . At these temperatures

(1) A. E. Finholt, A. C. Bond, and H. F. Schlesinger, *J. Amer. Chem. Soc.*, **69**, 1199 (1947).

(2) H. I. Schlesinger, H. C. Brown, H. R. Hoekstra, and L. R. Rapp, *J. Amer. Chem. Soc.*, **75**, 199 (1953).

(3) E. C. Ashby, R. Kovar, and R. Arnott, *J. Amer. Chem. Soc.*, **92**, 2182 (1970).

(4) E. C. Ashby, and R. D. Schwartz, *Inorg. Chem.*, **10**, 355 (1971).

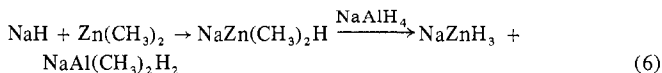
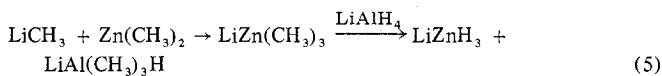
(5) E. C. Ashby, R. Kovar, and R. Arnott, *J. Amer. Chem. Soc.*, **92**, 2182 (1970).

(6) G. E. Coates and J. A. Heslop, *J. Chem. Soc. A*, 514 (1968).

(7) W. E. Becker and E. C. Ashby, *J. Org. Chem.*, **29**, 954 (1964).

(8) E. C. Ashby and R. G. Beach, *Inorg. Chem.*, **10**, 2486 (1971).

MZnR₂H and MZnR₃ compounds should not cleave ether solvents. Second, dimethylzinc could be used as a starting material rather than di-*sec*-butylzinc since methyl group exchange should be more rapid than *sec*-butyl group exchange (eq 5 and 6). In addition, Shriver and coworkers,⁹ in their



report on the preparation and properties of MZnR₂H compounds, showed that LiZn(CH₃)₂H and NaZn(CH₃)₂H are better defined species in solution than the higher alkyl analogs.

The advantages of using this method for preparation of complex metal hydrides of zinc are as follows: (1) the reactions are instantaneous and quantitative, (2) no ether cleavage products are formed, (3) high-pressure hydrogenation is not required, and (4) methyl-metal compounds in ether are much easier to prepare than the *sec*-butyl compounds in hydrocarbon solvent.

Experimental Section

Apparatus. Reactions were performed under nitrogen at the bench using Schlenk tube techniques. Filtrations and other manipulations were carried out in a glove box equipped with a recirculating system using manganese oxide columns to remove oxygen and Dry Ice-acetone to remove solvent vapors.¹⁰

Infrared spectra were obtained using a Perkin-Elmer 621 spectrophotometer. Solids were run as Nujol mulls between CsI plates. Solutions were run in matched 0.10-mm path length NaCl cells. X-Ray powder data were obtained on a Philips-Norelco X-ray unit using a 114.6-mm camera with nickel-filtered Cu K α radiation. Samples were sealed in 0.5-mm capillaries and exposed to X-rays for 6 hr. *d* spacings were read on a precalibrated scale equipped with viewing apparatus. Intensities were estimated visually. A 300-ml Magna-Drive autoclave (Autoclave Engineers, Inc.) was used for high-pressure hydrogenation. Dta-tga data were obtained under vacuum with a modified Mettler thermoanalyzer II. A diagram of the vacuum line attached to the balance chamber is shown in Figure 1. Operation of the dta-tga under vacuum with the U trap between R₁ and the pump cooled to liquid nitrogen temperature permits one to distinguish between condensable and noncondensable evolved gases by use of the gauges J₁ and J₂. The U-shaped tube can also be used as an analytical device to separate the condensed gases after the desired temperature limit has been reached. After the liquid nitrogen has been removed, slow warming of the copper branch produces a vertical thermal gradient which assures a good separation of the trapped products, the more volatile ones escaping first. The vacuum line was constructed to allow the use of the dta-tga under various conditions: vacuum, static pressure, or gas flow. In the latter case, the gas enters the chamber by V and leaves through r₁ or r₂ and r₃; R₂ open, R₁ closed.¹¹

Analytical. Gas analyses were carried out by hydrolyzing samples with hydrochloric acid on a standard vacuum line equipped with a Toepler pump.¹⁰ Methane in the presence of hydrogen was determined by volume in a tensimeter. Alkali metals were determined by flame photometry. Aluminum was determined by EDTA titration. Zinc in the presence of aluminum was determined by masking the aluminum with triethanolamine and titrating the zinc with EDTA. Zinc alone was determined by EDTA titration. Halogens were determined by the Volhard procedure.

Materials. Potassium and sodium hydride were obtained from Alfa Inorganics as a slurry in mineral oil. Lithium hydride was prepared by hydrogenolysis of *tert*-butyllithium at 4000 psig for 24 hr. Solutions of lithium and sodium aluminum hydride (Ventron, Metal Hydride Division) were prepared in both diethyl ether and tetrahy-

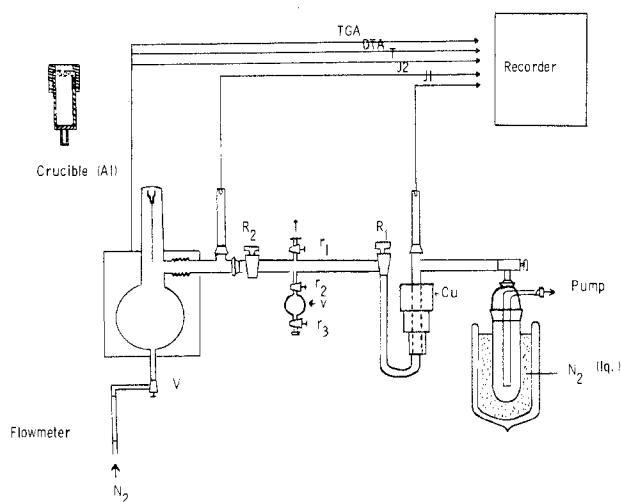


Figure 1. Description of high-vacuum portion of Mettler thermoanalyzer II.

drofuran in the usual manner. Dimethyl- and di-*sec*-butylzinc were prepared by the procedure of Noller.¹² Methyl and *sec*-butyl iodides were obtained from Fisher Scientific Co. The iodides were dried over anhydrous MgSO₄ and distilled prior to use. Zinc-copper couple was obtained from Alfa Inorganics. The reactions of zinc-copper couple with methyl iodide were allowed to proceed overnight. The dimethylzinc was distilled from the reaction mixture at atmospheric pressure under nitrogen while di-*sec*-butylzinc was distilled at reduced pressure. Methyl lithium (made from CH₃Cl) was obtained as a 5% solution in ether from Matheson Coleman and Bell and stored at -20° until ready to use. Tetrahydrofuran and benzene (Fisher Certified Reagent Grade) were distilled under nitrogen over NaAlH₄ and diethyl ether (Fisher Reagent) over lithium aluminum hydride. Ultrapure hydrogen (99.9995%) obtained from the Matheson Corp. was used for hydrogenation experiments. Alane was prepared by the reaction of 100% H₂SO₄ with LiAlH₄ in THF. Li₂SO₄ was removed by filtration and a lithium-free solution of AlH₃ in THF was obtained.¹³

Reactions Involving (*sec*-C₄H₉)₂Zn. (a) **Reaction of LiH and (*sec*-C₄H₉)₂Zn in Benzene.** Di-*sec*-butylzinc (66 mmol) in benzene was added to a slurry of LiH (66 mmol) in benzene. The mixture was filtered after it had been stirred for 1 week. The filtrate showed a Zn:*sec*-butyl ratio of 1:1.98, but no lithium or hydridic hydrogen was found. Analysis of the solid showed a Li:Zn:H ratio of 10:1:7.

(b) **Reaction of LiH and (*sec*-C₄H₉)₂Zn in THF.** Di-*sec*-butylzinc (27.9 mmol) in THF was added to 27.9 mmol of a LiH slurry in THF. The mixture was stirred at room temperature overnight. A clear solution resulted which exhibited a Li:Zn:*sec*-C₄H₉:H ratio of 1.00:0.96:1.88:0.32. Gas chromatography of the hydrolysate showed a large butanol peak due to extensive THF cleavage. A similar reaction was carried out in such a way that all of the THF was removed under vacuum immediately after the lithium hydride dissolved, but the lithium di-*sec*-butylhydrido zincate complex decomposed to lithium hydride and di-*sec*-butylzinc under vacuum. Thus, it was not possible to remove all the THF and dissolve the residue in a noncleaving solvent, such as benzene.

(c) **Reaction of LiH and (*sec*-C₄H₉)₂Zn in Diethyl Ether.** Di-*sec*-butylzinc (28 mmol) in diethyl ether was added to a slurry of 28 mmol of LiH in diethyl ether. The mixture was stirred for 1 week and filtered. The filtrate showed a Li:Zn ratio of 0.20:1.00. The solid exhibited a Li:Zn:H ratio of 1.00:0.06:0.97. The reaction was repeated under reflux conditions for 2 weeks. Still little reaction occurred.

(d) **Reaction of LiZn(*sec*-C₄H₉)₂H with LiAlH₄ in THF. Preparation of Li₂ZnH₄.** LiH (5.49 mmol) slurry in THF was added to 5.49 mmol of di-*sec*-butylzinc in THF. This mixture was stirred until all the lithium hydride dissolved (about 21 hr), then 8.11 mmol of LiAlH₄ in THF was added rapidly. After 5 min a white solid began to appear, and after 30 min the mixture had a slightly gray, thick, milky appearance. The mixture was stirred overnight at room temperature. The solid, now having a gray appearance, was separated by filtration and dried at room temperature *in vacuo*. *Anal.* Calcd for

(9) G. J. Kubas and D. F. Shriver, *J. Amer. Chem. Soc.*, **92**, 1949 (1970).

(10) D. F. Shriver, "The Manipulations of Air-Sensitive Compounds," McGraw-Hill, New York, N. Y., 1969.

(11) E. C. Ashby, P. Claudy, and Bousquet, *J. Chem. Educ.*, in press.

(12) C. R. Noller, *Org. Syn.*, **12**, 86 (1932).

(13) H. C. Brown and N. M. Yoon, *J. Amer. Chem. Soc.*, **88**, 1464 (1966).

Li_2ZnH_4 : Li, 16.7; Zn, 78.5; H, 4.85. Found: Li, 16.3; Zn, 79.5; H, 4.11. The molar ratio of Li:Zn:H is 1.93:1.00:3.36. The filtrate contained 8.50 mmol of aluminum, 3.40 mmol of zinc, and 10.31 mmol of lithium. The amount of Li_2ZnH_4 recovered was 2.09 mmol of a theoretical 2.75 mmol. The X-ray powder diffraction data are given in Table I. The infrared spectrum of the solid product (Nujol mull) showed two strong broad bands at 400–1000 cm^{-1} centered at 650 cm^{-1} and 1200–1650 cm^{-1} centered at 1450 cm^{-1} . This spectrum was very similar to that found for K_2ZnH_4 .⁸

Reactions Involving $(\text{CH}_3)_2\text{Zn}$ and LiH . (a) Reaction of $\text{LiZn}(\text{CH}_3)_2\text{H}$ with LiAlH_4 in THF. Attempted Preparation of LiZnH_3 . Dimethylzinc (10 mmol) in THF was added to 10 mmol of LiH slurry in THF. After 5 hr of stirring the solution was clear. LiAlH_4 (10 mmol) in THF was added quickly. After 1 min the solution became faintly cloudy, and after 30 min a thick white mixture was present. The mixture was stirred overnight at room temperature and filtered the next day. The precipitate, which had now become very gray due to decomposition to zinc metal, was dried at room temperature *in vacuo*. Anal. Calcd for LiZnH_3 : Li, 9.2; Zn, 86.8; H, 4.0. Found: Li, 9.4; Zn, 87.2; H, 3.35. The molar ratio of Li:Zn:H was 1.00:1.00:2.51. The filtrate contained 10.78 mmol of aluminum, 1.41 mmol of zinc, and 11.20 mmol of lithium. The amount of solid recovered was 8.59 mmol of a theoretical 10 mmol. The X-ray powder diffraction data which are given in Table I showed lines for Li_2ZnH_4 and zinc metal only.

(b) Reaction of LiH and $(\text{CH}_3)_2\text{Zn}$ in 2:1 Ratio in THF. Attempted Preparation of $\text{Li}_2\text{Zn}(\text{CH}_3)_2\text{H}_2$. Lithium hydride slurry (20 mmol) in THF was added to 10 mmol of dimethylzinc in THF. The resulting mixture was stirred for 2 weeks at room temperature. A solid was always present. The solid was separated by filtration and dried at room temperature *in vacuo*. The solid had a molar ratio of Li:Zn of 15.22:1.00. The X-ray powder diffraction pattern of the solid product contained lines due to lithium hydride and zinc metal only. The Li:Zn ratio of the filtrate was 1.28:1.00.

(c) Reaction of $\text{LiZn}_2(\text{CH}_3)_2\text{H}$ with LiAlH_4 in THF. Attempted Preparation of LiZn_2H_5 . Lithium hydride slurry (5 mmol) in THF was added to 10 mmol of dimethylzinc in THF. Within 5 min a clear solution resulted. After addition of 20 mmol of LiAlH_4 an infrared spectrum of the solution showed only bands due to LiAlH_4 . After 30 min some gray solids began to appear. The mixture was stirred overnight at room temperature. The next day, very gray, almost black solids were present. The precipitate was separated by filtration and dried at room temperature *in vacuo*. The molar ratio of Li:Zn:H in the solid was 1.00:2.06:2.96. The filtrate contained 20.20 mmol of aluminum, 1.02 mmol of zinc, and 19.60 mmol of lithium. The gas evolved on hydrolysis of the filtrate was found to contain hydrogen to methane in the molar ratio 4.28:1.00. The infrared spectrum of the filtrate corresponded to a mixture of $\text{LiAl}(\text{CH}_3)_2\text{H}_2$ and LiAlH_4 . X-Ray powder diffraction data for the solid which are given in Table I showed lines for Li_2ZnH_4 and zinc metal only. Infrared analysis (Nujol mull) of the solid showed three broad bands (400–700, 950–1150, and 1350–2000 cm^{-1}).

Reactions Involving $(\text{CH}_3)_2\text{Zn}$ with CH_3Li . (a) Reaction of LiAlH_4 with $\text{LiZn}(\text{CH}_3)_3$ in Diethyl Ether. Preparation of LiZnH_3 . Methylolithium (5 mmol) in diethyl ether were added to 5 mmol of dimethylzinc in diethyl ether. The resulting solution was stirred at room temperature for 1 hr; then 7.5 mmol of LiAlH_4 in diethyl ether was added. A white precipitate appeared immediately. This mixture was stirred at room temperature for another hour and filtered. The white solid was dried at room temperature *in vacuo* and analyzed. Anal. Calcd for LiZnH_3 : Li, 9.2; Zn, 86.8; H, 4.0. Found: Li, 9.2; Zn, 86.5; H, 4.30. The molar ratio of Li:Zn:H was 1.00:1.00:3.21. The filtrate contained 7.53 mmol of aluminum, no zinc, and 7.34 mmol of lithium. The amount of LiZnH_3 recovered was 5 mmol of a theoretical 5 mmol. The X-ray powder diffraction data are given in Table I.

(b) Reaction of LiAlH_4 with $\text{Li}_2\text{Zn}(\text{CH}_3)_4$ in Diethyl Ether. Preparation of Li_2ZnH_4 . Dimethylzinc (10 mmol) in diethyl ether was added to 20 mmol of methylolithium in diethyl ether. The resulting solution was stirred for 1 hour at room temperature, followed by addition of 20 mmol of LiAlH_4 in diethyl ether. White solids appeared immediately; however, the mixture was stirred for an additional 1 hr at room temperature, filtered, and dried *in vacuo*. Anal. Calcd for Li_2ZnH_4 : Li, 16.7; Zn, 78.5; H, 4.85. Found: Li, 14.8; Zn, 80.4; H, 4.85. The molar ratio of Li:Zn:H was 1.73:1.00:3.94. The filtrate contained 19.30 mmol of aluminum, no zinc, and 20.01 mmol of lithium. The amount of Li_2ZnH_4 recovered was 10 mmol of a theoretical 10 mmol. The X-ray powder diffraction data are given in Table I. Infrared analysis (Nujol mull) showed three broad bands [400–900, 1200–1400 (centered at 1290 cm^{-1}), and 1400–1900

cm^{-1} (centered at 1580 cm^{-1})]. Infrared analysis of the filtrate (KBr cell, 0.10-mm path length) showed a strong peak in the Al-H stretching region centered at 1700 cm^{-1} and a moderate peak in the Al-H deformation region centered at 760 cm^{-1} . This spectrum is characteristic of the species $\text{LiAl}(\text{CH}_3)_2\text{H}_2$.

(c) Reaction of LiAlH_4 with $\text{Li}_3\text{Zn}(\text{CH}_3)_3$ in Diethyl Ether. Preparation of Li_3ZnH_5 . Methylolithium (15 mmol) in diethyl ether was added to 5 mmol of dimethylzinc in diethyl ether. The resulting solution was stirred for 1 hr at room temperature, followed by addition of 12.5 mmol of LiAlH_4 in diethyl ether. A white precipitate appeared immediately. The mixture was stirred for an additional hour at room temperature and then filtered. The resulting white solid was dried at room temperature *in vacuo* and analyzed. Anal. Calcd for Li_3ZnH_5 : Li, 22.9; Zn, 71.6; H, 5.53. Found: Li, 20.8; Zn, 71.5; H, 5.47; Al, 2.01. The molar ratio of Li:Zn:H: LiAlH_4 was 2.67:1.00:4.88:0.068. The filtrate contained 11.92 mmol of aluminum, no zinc, and 13.42 mmol of lithium. The molar ratio of Li:Al:Zn in the filtrate was 1.12:1.00:0.00. The amount of Li_3ZnH_5 recovered was 5 mmol of a theoretical 5 mmol. The X-ray powder diffraction data are given in Table I. Infrared analysis of the solid (Nujol mull) showed two strong bands at 400–950 (centered at 680 cm^{-1}) and 1400–1900 cm^{-1} (centered at 1500 cm^{-1}) and two moderate bands at 950–1100 (centered at 990 cm^{-1}) and 1150–1450 cm^{-1} (centered at 1280 cm^{-1}).

(d) Reaction of LiAlH_4 with $\text{LiZn}_2(\text{CH}_3)_2$ in Diethyl Ether. Attempted Preparation of LiZn_2H_5 . Methylolithium (5 mmol) in diethyl ether was added to 10 mmol of dimethylzinc in diethyl ether. The resulting solution was stirred for 1 hr at room temperature; 12.5 mmol of LiAlH_4 in diethyl ether was added. A white precipitate appeared immediately. This mixture was then stirred for an additional hour and filtered. The solid which was slightly gray at this point was dried under vacuum at room temperature. Anal. Calcd for LiZn_2H_5 : Li, 4.86; Zn, 91.6; H, 3.54. Found: Li, 5.08; Zn, 91.6; H, 3.45. The molar ratio of Li:Zn:H was 1.00:1.92:4.66. The filtrate contained 12.55 mmol of aluminum, 0.04 mmol of zinc, and 12.59 mmol of lithium. The amount of solid recovered was 5 mmol of a theoretical 5 mmol. The X-ray powder diffraction data are given in Table I.

(e) Reaction of LiAlH_4 with $\text{LiZn}_3(\text{CH}_3)_3$ in Diethyl Ether. Attempted Preparation of LiZn_3H_7 . Dimethylzinc (15 mmol) in diethyl ether was added to 5 mmol of methylolithium in diethyl ether. The resulting solution was stirred for 1 hr at room temperature followed by addition of 17.5 mmol of LiAlH_4 in diethyl ether. A white precipitate appeared immediately. This mixture was stirred for 1 hr and filtered. The solid, which had turned slightly gray, was dried under vacuum at room temperature. Anal. Calcd for LiZn_3H_7 : Li, 3.30; Zn, 93.4; H, 3.36. Found: Li, 3.11; Zn, 93.6; H, 3.34. The molar ratio of Li:Zn:H was 1.00:3.20:7.37. The filtrate contained 18.02 mmol of aluminum, no zinc, and 18.20 mmol of lithium. The yield of solid was 100%. The X-ray powder diffraction data are given in Table I.

Reactions Involving $(\text{CH}_3)_2\text{Zn}$ with KH . (a) Reaction of KH (Excess) and $(\text{CH}_3)_2\text{Zn}$ in Diethyl Ether. Dimethylzinc (26.73 mmol) in diethyl ether was added to a slurry of 60.4 mmol of potassium hydride in diethyl ether. The slurry became hot immediately and solvent came to reflux. A solid was always present during the reaction. The mixture was stirred overnight at room temperature and filtered the next day. The resulting white solid was dried under vacuum at room temperature. The X-ray powder diffraction data are given in Table II. The filtrate showed a molar ratio of K:Zn of 0.92:1.00, but it contained only 0.59 mmol of zinc; *i.e.*, only 2.22% of the starting zinc was found in the filtrate. The solid was slurried for 3 hr in THF and then filtered. The residual solid was shown to be KH by X-ray powder diffraction and the filtrate had a molar ratio of K:Zn: CH_3 :H of 0.98:1.00:2.14:0.39. The $\text{KZn}(\text{CH}_3)_2\text{H}$ formed cleaved THF at room temperature producing a soluble product.

(b) Reaction of AlH_3 with $\text{KZn}(\text{CH}_3)_2\text{H}$ in THF. Preparation of KZn_2H_5 . Dimethylzinc (10 mmol) in THF was added to 10 mmol of a slurry of KH in THF at room temperature. The mixture was clear within 1 min. The mixture was quickly cooled to -80° to prevent ether cleavage and stirred an additional 2 hr. Next, 10 mmol of AlH_3 in THF was added at -80° . The bath was removed and the reaction mixture allowed to warm to room temperature. After 15 min a white precipitate began to form. The mixture was stirred an additional hour and filtered. The solid was dried under vacuum at room temperature. Anal. Calcd for KZn_2H_5 : K, 22.4; Zn, 74.8; H, 2.88. Found: K, 23.2; Zn, 74.0; H, 2.79. The molar ratio of K:Zn: CH_3 :H was 1.05:2.00:0.00:4.92. The filtrate contained 10.21 mmol of aluminum, no zinc, and 5.26

Table I. X-Ray Powder Patterns for Complex Metal Zinc Hydrides of Lithium

$\text{Li}_2\text{ZnH}_4 + \text{Zn}^a$		$\text{Li}_2\text{ZnH}_4 + \text{Zn}^b$		$\text{Li}_2\text{ZnH}_4 + \text{Zn}^c$		$\text{Li}_2\text{ZnH}_4^d$		$\text{Li}_3\text{ZnH}_5^e$		$\text{Li}_2\text{ZnH}_3^f$		${}^{11}\text{LiZn}_2\text{H}_3^g$		${}^{11}\text{LiZn}_3\text{H}_7^h + \text{Zn}^i$		LiH^j		ZnH_2^k	
d, Å	l/l_0	d, Å	l/l_0	d, Å	l/l_0	d, Å	l/l_0	d, Å	l/l_0	d, Å	l/l_0	d, Å	l/l_0	d, Å	l/l_0	d, Å	l/l_0	d, Å	l/l_0
4.25	m	4.25	m	4.22	mw	5.02	m	4.45	w	6.25	m	6.24	m	6.24	m	4.51	vw	4.51	vw
3.83	m	3.85	m	3.85	w	4.69	w	2.84	s	5.02	w	4.45	s	4.45	s	4.23	s	4.23	s
3.67	w	3.69	mw	3.69	w	4.25	s	2.78	w	4.45	vs	4.30	m	3.24	m	3.80	vw	3.80	vw
3.44	m	3.44	m	3.42	w	3.84	vs	2.64	m	4.30	m	3.26	s	3.10	m	3.40	m	3.40	m
2.95	m	2.95	m	3.25	vw	3.65	m	2.50	m	4.19	m	3.10	m	2.91	mw	2.97	vw	2.97	vw
2.70	w	2.68	mw	2.95	mw	3.42	ms	1.91	w	3.81	ms	2.94	m	2.81	m	2.828	vw	2.828	vw
2.47	w	2.46	ms	2.73	w	2.95	ms	1.79	w	3.65	w	2.81	m	2.45	m	2.608	w	2.608	w
2.43	m	2.29	ms	2.46	ms	2.71	mw	1.63	mw	3.42	mw	2.50	m	2.31	mw	2.468	vw	2.468	vw
2.29	w	2.09	vs	2.29	ms	2.46	s	1.50	m	3.24	vs	2.41	m	2.16	mw	2.387	m	2.387	m
2.12	w	1.90	vw	2.09	s	2.42	s	1.385	w	3.10	m	2.24	w	2.09	s	2.290	m	2.290	m
2.08	m	1.83	vw	1.68	m	2.32	m			2.94	s	2.17	mw	1.98	w	2.225	m	2.225	m
1.95	w	1.68	m	1.34	m	2.26	mw			2.81	s	2.07	w	1.96	w	2.135	w	2.135	w
1.84	w	1.33	m	1.33	m	2.24	mw			2.50	mw	1.98	w	1.75	w	2.085	w	2.085	w
1.68	w	1.23	w	1.23	w	2.12	m			2.45	m	1.95	w	1.68	w	2.017	vw	2.017	vw
1.60	w	1.17	m	1.17	m	2.07	w			2.41	m	1.75	w	1.33	w	1.905	w	1.905	w
1.17	w	1.15	w	1.15	w	1.99	m			2.31	w	1.60	w	1.17	w	1.764	w	1.764	w
0.90	w	1.12	m	1.12	m	1.91	m			2.24	mw	1.495	w	1.12	w	1.688	vw	1.688	vw
0.865	w	1.09	w	1.09	w	1.84	m			2.16	mw	1.25	vw			1.603	vw	1.603	vw
		1.04	w	1.04	w	1.79	m			2.12	w					1.562	vw	1.562	vw
		0.941	w	0.941	w	1.70	w			2.06	w					1.486	vw	1.486	vw
		0.907	w	0.907	w	1.67	w			1.98	mw					1.464	vw	1.464	vw
		0.904	w	0.905	w	1.64	w			1.94	mw					1.416	vw	1.416	vw
		0.903	w	0.870	w	1.60	m			1.90	mw					1.336	vw	1.336	vw
		0.870	w	0.856	w	1.57	w			1.84	w					1.305	vw	1.305	vw
		0.856	w	0.855	w	1.54	w			1.75	mw					1.295	vw	1.295	vw
		0.854	w	0.821	w	1.52	w			1.64	w					1.259	vw	1.259	vw
		0.821	w	0.819	w	1.50	w			1.60	m					1.219	vw	1.219	vw
		0.818	w			1.48	m			1.52	w					1.172	vw	1.172	vw
						1.47	M			1.495	w					1.157	vw	1.157	vw
						1.44	w			1.44	w					1.123	vw	1.123	vw
						1.456	w			1.244	w								
						1.397	w												
						1.36	w												
						1.34	w												
						1.32	w												
						1.29	w												
						1.21	w												

^a $\text{LiZn}(\text{sec-C}_4\text{H}_9)_2\text{H} + \text{LiAlH}_4$ in THF. ^b $\text{LiZn}(\text{CH}_3)_2\text{H} + \text{LiAlH}_4$ in THF. ^c $\text{LiZn}_2(\text{CH}_3)_4\text{H} + \text{LiAlH}_4$ in THF. ^d $\text{Li}_2\text{Zn}(\text{CH}_3)_2 + \text{LiAlH}_4$ in diethyl ether. ^e $\text{Li}_3\text{Zn}(\text{CH}_3)_5 + \text{LiAlH}_4$ in diethyl ether. ^f $\text{LiZn}(\text{CH}_3)_3 + \text{LiAlH}_4$ in diethyl ether. ^g $\text{LiZn}_2(\text{CH}_3)_5 + \text{LiAlH}_4$ in diethyl ether. ^h $\text{LiZn}_3(\text{CH}_3)_7 + \text{LiAlH}_4$ in diethyl ether. ⁱ ASTM file. ^j ASTM file. ^k $\text{LiAlH}_4 - (\text{C}_2\text{H}_5)_2\text{Zn}$, see ref 5. ^l w, weak; m, medium; s, strong; v, very.

Table II. X-Ray Powder Patterns for Complex Metal Zinc Hydrides of Potassium

KZn(CH ₃) ₂ + KH ^a		KH ^b		K ₂ ZnH ₄ ^c		ZnH ₂ ^d		KZn ₂ H ₅ ^e		KZn ₂ H ₅ ^f		"KZn ₃ H ₇ " ^g		KZnH ₃ ^h	
d, Å	I/I ₀ ⁱ	d, Å	I/I ₀	d, Å	I/I ₀	d, Å	I/I ₀	d, Å	I/I ₀	d, Å	I/I ₀	d, Å	I/I ₀	d, Å	I/I ₀
6.10	mw			5.10	w	4.51	vw	6.03	s	6.03	s	6.02	ms	6.25	ms
5.30	mw			4.26	m	4.23	s	4.10	mw	4.08	mw	4.06	mw	5.60	vw
4.05	mw, d			3.89	w	3.80	vw	3.72	mw	3.72	w	3.72	w	5.10	s
3.89	mw, d			3.62	vw	3.40	m	3.36	vs	3.36	vs	3.36	vw	4.40	vw
3.59	ms, d			3.47	m	2.97	vw	3.01	m	3.02	mw	3.02	mw	3.71	vw
3.40	ms, d			3.24	w	2.828	vw	2.67	vw	2.69	w	2.79	vw	3.59	m
3.27	s	3.30	vs	3.09	s	2.608	w	2.59	vw	2.61	w	2.69	vw	3.43	vs
2.83	s	2.86	s	2.940	s	2.468	vw	2.42	s	2.43	s	2.60	vw	3.31	m
2.75	w			2.744	w	2.387	m	2.35	s	2.34	s	2.43	s	3.11	ms
2.45	m			2.568	vw	2.290	m	2.18	m	2.18	m	2.35	s	2.80	s
2.10	w			2.354	w	2.225	m	2.14	vw	2.02	w	2.28	vw	2.71	vs
2.00	ms			2.128	w	2.135	w	2.00	vw	1.93	ms	2.19	m	2.58	s
1.71	ms	1.72	s	1.946	w	2.085	w	1.93	ms	1.85	m	2.09	m	2.33	s
1.64	w	1.65	m	1.814	w	2.017	vw	1.85	m	1.80	m	2.03	vw	2.29	w
1.57	vw			1.734	w	1.905	w	1.80	m	1.68	m	2.01	vw	2.18	w
1.43	w	1.43	m	1.648	vw	1.764	w	1.68	m	1.53	w	1.93	ms	2.15	vw
1.30	w	1.31	m	1.624	vw	1.688	vw	1.54	w	1.490	m	1.86	m	2.12	vw
1.27	w	1.28	m	1.571	w	1.630	vw	1.49	m	1.432	w	1.81	m	2.07	m
1.16	w	1.17	m	1.488	w	1.562	vw	1.431	w	1.415	w	1.69	m	2.03	w
1.09	w	1.10	m	1.470	w	1.486	vw	1.414	w	1.371	w	1.65	vw	1.94	vw
0.96	w	1.01	w	1.384	vw	1.464	vw	1.371	mw	1.351	w	1.53	vw	1.90	ms
				1.213	w	1.416	vw	1.355	mw	1.322	w	1.49	m	1.86	w
						1.336	vw	1.328	w	1.270	w	1.435	mw	1.85	vw
						1.305	vw	1.269	vw	1.234	vw	1.419	w	1.79	m
						1.295	vw	1.238	vw	1.222	w	1.361	mw	1.77	m
						1.219	vw	1.222	w	1.191	vw	1.355	mw	1.73	m
						1.172	vw	1.176	w	1.175	w	1.321	vw	1.72	w
						1.157	vw	1.151	vw	1.154	vw	1.300	vw	1.69	m
						1.123	vw	1.111	w	1.111	w	1.271	vw	1.66	w
						1.042	vw	1.076	vw	1.078	w	1.239	vw	1.64	w
								1.060	vw	1.057	w	1.223	w	1.595	m
								1.005	vw	1.003	vw	1.221	vw	1.57	w
								0.983	vw	0.986	vw	1.175	vw	1.55	w
								0.922	vw	0.922	vw	1.152	vw	1.455	mw
								0.888	vw	0.906	vw	1.111	w	1.370	mw
											1.079	w	1.325	mw	
											1.059	w			

^a Excess KH + (CH₃)₂Zn in diethyl ether. ^b ASTM files. ^c KH + (sec-C₄H₉)₂Zn in benzene, see ref 5. ^d LiAlH₄ + (C₂H₅)₂Zn, see ref 5. ^e KZn(CH₃)₂H + AlH₃ in tetrahydrofuran. ^f KZn₂(CH₃)₂H + AlH₃ in tetrahydrofuran. ^g KZn₃(CH₃)₆ + AlH₃ in tetrahydrofuran. ^h KZn(CH₃)₂H + LiAlH₄ in tetrahydrofuran. ⁱ w, weak; m, medium; s, strong; v, very; d, diffused.

mmol of potassium. The molar ratio of K:Al in the filtrate was 1.03:2.00. The X-ray powder diffraction pattern of the solid is given in Table II.

(c) Reaction of LiAlH₄ with KZn(CH₃)₂H in THF. Preparation of KZnH₃. Dimethylzinc (10 mmol) in THF was added to 10 mmol of KH slurried in THF. The clear solution which resulted was cooled to -80° and stirred for 1 hr. Next, 10 mmol of lithium aluminum hydride in THF was added to the solution. The solution was warmed to room temperature and a white precipitate resulted. This mixture was stirred for 1 hr and filtered. The resulting white solid was dried under vacuum at room temperature. *Anal.* Calcd for KZnH₃: K, 36.4; Zn, 60.8; H, 2.81. Found: K, 36.6; Zn, 60.5; H, 2.86. The molar ratio of Li:K:Zn:H was 0.00:1.01:1.00:2.96. The filtrate contained 9.64 mmol of aluminum, no zinc, no potassium, and 9.75 mmol of lithium. The molar ratio of K:Li:Al in the filtrate was 0.00:1.01:1.00. The X-ray powder diffraction pattern of the solid is given in Table II.

(d) Reaction of AlH₃ with KZn₂(CH₃)₂H in THF. Preparation of KZn₂H₅. Dimethylzinc (20 mmol) in THF was added to 10 mmol of KH slurried in THF. A clear solution resulted even before all the dimethylzinc could be introduced. The solution was quickly cooled to -80° and stirred for an additional hour at this temperature. Next, 14.82 mmol of AlH₃ in THF was added to the solution at -80°. A faint white precipitate appeared immediately. The bath was removed and the mixture stirred for 1 hr and then filtered. The solid was dried under vacuum at room temperature. *Anal.* Calcd for KZn₂H₅: K, 22.4; Zn, 74.8; H, 2.88. Found: K, 21.5; Zn, 75.8; H, 2.79. The molar ratio of K:Zn:H was 1.00:2.10:5.04. The filtrate contained 16.96 mmol of aluminum, no zinc, and 0.83 mmol of potassium. The molar ratio of K:Al in the filtrate was 0.098:2.00. The X-ray powder diffraction pattern of the solid is given in Table II.

(e) Reaction of AlH₃ with KZn₂(CH₃)₂H in THF. Attempted Preparation of KZn₃H₇. Dimethylzinc (15 mmol) in THF was added to 5 mmol of KH slurried in THF. The clear solution which resulted was cooled to -80° and stirred for 1 hr. Next, 15 mmol of AlH₃ in THF was added to the solution at -80°. The mixture was allowed to warm to room temperature (a white precipitate formed in the process), stirred for 1 hr, and then filtered. The solid was dried under vacuum at room temperature. *Anal.* Calcd for KZn₃H₇: K, 16.1; Zn, 80.9; H, 2.92. Found: K, 15.0; Zn, 82.1; H, 2.92. The molar ratio of K:Zn:H was 1.00:3.29:7.56. The filtrate contained 16.09 mmol of aluminum, no zinc, and 0.44 mmol of potassium. The molar ratio of K:Al in the filtrate was 0.055:2.00. The X-ray diffraction pattern of the solid, which is given in Table II, showed lines due to KZn₂H₅ only.

Reactions Involving (CH₃)₂Zn with NaH. (a) Reaction of NaAlH₄ with NaZn(CH₃)₂H in THF. Preparation of NaZnH₃. Dimethylzinc (10 mmol) in THF was added to 10 mmol of NaH slurried in THF. The mixture was quickly cooled to -80° and stirred at that temperature until the Na:Zn ratio in the supernatant was 1:1. At this point, 5 mmol of the supernatant solution [NaZn(CH₃)₂H] was allowed to react with 5 mmol of sodium aluminum hydride in THF. A white precipitate appeared within minutes. The mixture was stirred 20 min and filtered. The resulting white solid was dried under vacuum at room temperature. *Anal.* Calcd for NaZnH₃: Na, 25.2; Zn, 71.5; H, 3.30. Found: Na, 25.2; Zn, 71.6; H, 3.24. The molar ratio of Na:Zn:H was 1.00:1.00:2.94. The X-ray powder diffraction pattern is given in Table III. The filtrate contained 4.62 mmol of aluminum, 0.47 mmol of zinc, and 5.06 mmol of sodium.

(b) Reaction of AlH₃ and NaZn(CH₃)₂H in THF. Preparation of NaZn₂H₅. Dimethylzinc (5 mmol) in THF was added to 5 mmol of a slurry of NaH in THF at room temperature. Quickly, 5 mmol

of AlH_3 in THF was added at room temperature. An off-white precipitate appeared. The mixture was stirred for 2 hr and filtered. The solid was dried under vacuum at room temperature. *Anal.* Calcd for NaZn_2H_5 : Na, 14.5; Zn, 82.4; H, 3.15. Found: Na, 15.2; Zn, 81.7; H, 3.01. The molar ratio of Na:Zn:H was 1.06:2.00:4.83. The molar ratio of Na:Al:Zn in the filtrate was 1.03:2.00:0.061. The X-ray powder diffraction pattern of the solid is given in Table III.

(c) **Reaction of $\text{NaZn}(\text{CH}_3)_2\text{H}$ with LiAlH_4 in THF. Preparation of NaZnH_3 .** To 6 mmol of $\text{NaZn}(\text{CH}_3)_2\text{H}$ in THF at -80° was added 6 mmol of LiAlH_4 in THF. This mixture was allowed to warm to room temperature during which time a white precipitate resulted. The resulting white solid was filtered and dried at room temperature under vacuum. The molar ratio of Na:Zn:H in the solid was 1.00:1.00:2.75. The X-ray powder diffraction pattern, given in Table III, was identical with that of NaZnH_3 . The filtrate contained 5.82 mmol of aluminum and 3.04 mmol of zinc.

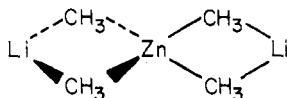
(d) **Reaction of NaAlH_4 with $\text{NaZn}_2(\text{CH}_3)_4\text{H}$ in THF. Attempted Preparation of NaZn_2H_5 .** Dimethylzinc (20 mmol) in THF was added to 10 mmol of NaH slurried in THF. The mixture was quickly cooled to -80° and stirred until the Na:Zn ratio in the supernatant was 0.50:1.00. At this point, 5 mmol of the supernatant [$\text{NaZn}_2(\text{CH}_3)_4\text{H}$ solution] was allowed to react with 10 mmol of sodium aluminum hydride in THF. A white precipitate appeared within minutes. The mixture was stirred for 1 hr and filtered. The resulting white solid was dried at room temperature under vacuum. The molar ratio of Na:Zn:H in the solid was 1.00:1.00:2.90. The X-ray powder diffraction pattern, given in Table III, was identical with that for NaZnH_3 . The filtrate contained 10.00 mmol of aluminum, 3.06 mmol of zinc, and 9.50 mmol of sodium.

(e) **Reaction of NaH with $(\text{sec-Bu})_2\text{Zn}$ in THF. Attempted Preparation of $\text{Na}_2\text{Zn}(\text{sec-C}_4\text{H}_9)_2\text{H}_2$ and Na_2ZnH_4 .** To 10 mmol of NaH slurried in THF was added 5 mmol of $(\text{sec-Bu})_2\text{Zn}$ in THF. The mixture was stirred at room temperature for 1 day (a solid remained throughout this period) and then filtered. The solid was dried under vacuum at room temperature. The molar ratio of Na:H:Zn in the solid was found to be 1.00:1.03:0.070. The X-ray powder diffraction pattern and vacuum dta-tga showed that the solid was mostly NaH. The filtrate, which contained sodium and zinc in a molar ratio of 1.11:1.00, when allowed to react with NaAlH_4 , yielded NaZnH_3 only.

Results and Discussion

While it is known that metal hydrides of the main group elements can be prepared by the reduction of a metal alkyl with lithium aluminum hydride,¹⁴ there have been no reports of the application of this simple reaction to the synthesis of new complex metal hydrides. When we found that the "ate" complexes of zinc [*i.e.*, $\text{LiZn}(\text{sec-C}_4\text{H}_9)_2\text{H}$] are cleaved by ether solvents, at the temperatures necessary to carry out hydrogenolysis ($75\text{--}150^\circ$) to the corresponding hydride, it was necessary to develop another method of reduction that could be carried out at lower temperature. It was found that LiAlH_4 , NaAlH_4 , or AlH_3 will reduce the "ate" complex to the corresponding hydride rapidly at room temperature.

Li_2ZnH_4 . The "ate" complex $\text{Li}_2\text{Zn}(\text{CH}_3)_4$, lithium tetramethylzincate, first prepared by Hurd¹⁵ in 1948, has been characterized both by nmr¹⁶ and X-ray crystallography.¹⁷ Its structure is shown below.



When $\text{Li}_2\text{Zn}(\text{CH}_3)_4$ and LiAlH_4 were allowed to react, Li_2ZnH_4 was obtained in 100% yield according to eq 7. The X-ray powder diffraction pattern of Li_2ZnH_4 (Table I)

(14) G. D. Barbaras, C. Dillard, A. E. Finholt, T. Wartick, K. E. Wilzbach, and H. I. Schlesinger, *J. Amer. Chem. Soc.*, **73**, 4585 (1951).

(15) D. J. Hurd, *J. Org. Chem.*, **13**, 711 (1948).

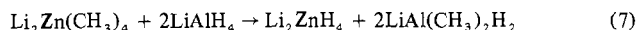
(16) L. M. Seitz and T. L. Brown, *J. Amer. Chem. Soc.*, **88**, 4140 (1966).

(17) E. Weiss and R. Wolfrum, *Chem. Ber.*, **101**, 35 (1968).

Table III. X-Ray Powder Patterns for Complex Metal Zinc Hydrides of Sodium

NaZnH_3^a		NaZnH_3^b		NaZnH_3^c		NaH^d		$\text{NaZn}_2\text{H}_5^e$	
<i>d</i> , Å	<i>I</i> / <i>I</i> ₀ ^f	<i>d</i> , Å	<i>I</i> / <i>I</i> ₀	<i>d</i> , Å	<i>I</i> / <i>I</i> ₀	<i>d</i> , Å	<i>I</i> / <i>I</i> ₀	<i>d</i> , Å	<i>I</i> / <i>I</i> ₀
8.70	vw	8.70	vw					5.84	m
5.99	w	5.99	w	5.87	vw			4.89	s
4.90	vs	4.90	vs	4.90	s			3.29	vs
4.39	w	4.40	w					3.09	m
3.98	w	3.91	w					2.83	s
3.30	m	3.52	w					2.50	w
3.11	vs	3.27	ms	3.26	m			2.44	m
2.91	m	3.11	vs	3.11	vs			2.36	m
2.81	w	2.92	m					2.26	m
2.63	mw	2.81	m	2.84	w	2.83	s	2.15	w
2.56	m	2.62	w					2.09	w
2.49	ms	2.56	ms					2.01	mw
2.43	m	2.49	s	2.51	m	2.44	ms	1.70	m
2.38	vw	2.44	m	2.45	w			1.62	w
2.26	w	2.25	w	2.38	vw			1.55	w
2.22	w	2.20	w	2.28	vw			1.50	w
2.15	w	2.15	vw	2.23	vw			1.465	w
2.07	w	2.07	w	2.16	vw			1.375	w
1.96	mw	2.02	vw	2.09	vw			1.351	w
1.83	mw	1.97	mw	2.02	vw			1.301	vw
1.78	w	1.84	w	1.98	w				
1.72	vw	1.78	w	1.79	vw	1.73	ms		
1.66	mw	1.70	w	1.70	vw	1.47	ms		
1.61	mw	1.66	w	1.67	vw	1.41	m		
1.58	vw	1.61	mw	1.62	w	1.22	mw		
1.53	mw	1.58	w	1.55	w	1.12	m		
1.49	vw	1.53	mw	1.47	vw	1.09	m		
1.38	vw	1.49	vw	1.35	vw	0.996	m		
1.34	w	1.47	vw			0.939	m		
1.22	vw	1.37	vw			0.863	mw		
1.06	vw	1.34	vw			0.825	m		
1.00	vw	1.22	vw			0.813	m		
		1.00	vw						

^a $\text{NaZn}(\text{CH}_3)_2\text{H} + \text{NaAlH}_4$ in tetrahydrofuran. ^b $\text{NaZn}(\text{CH}_3)_2\text{H} + \text{NaAlH}_4$ in tetrahydrofuran. ^c See ref 11, made by thermally decomposing $\text{NaZn}_2(\text{CH}_3)_4\text{H}_2$. ^d ASTM file. ^e $\text{NaZn}(\text{CH}_3)_2\text{H} + \text{AlH}_3$ in tetrahydrofuran. ^f w, weak; m, medium; s, strong; v, very.

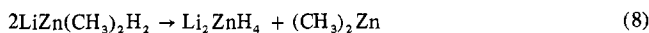


contains no lines due to LiH or ZnH_2 ; therefore, the product is not a physical mixture of the two simple hydrides. On the other hand, both the powder diffraction pattern and infrared spectrum of Li_2ZnH_4 were similar to that found for K_2ZnH_4 (Table II). The infrared spectrum of the solution that remained after filtration of Li_2ZnH_4 showed that the aluminum-containing species was $\text{LiAl}(\text{CH}_3)_2\text{H}_2$. Therefore, complete exchange of the methyl groups from zinc to aluminum had occurred. The structure of Li_2ZnH_4 might be similar to that of $\text{Li}_2\text{Zn}(\text{CH}_3)_4$, however, due to the insolubility of the hydride; association, ir, and nmr data are not available to establish this point.

Oddly enough, the reaction of either $\text{LiZn}(\text{sec-C}_4\text{H}_9)_2\text{H}$, $\text{LiZn}(\text{CH}_3)_2\text{H}$, or $\text{LiZn}_2(\text{CH}_3)_4\text{H}$ with LiAlH_4 in tetrahydrofuran also yields Li_2ZnH_4 . The X-ray powder diffraction patterns of Li_2ZnH_4 from each of these reactions (Table I) show weak to moderate lines for Li_2ZnH_4 and strong lines for zinc metal. It was found that the presence of a large excess of tetrahydrofuran with any of the complex metal hydrides discussed here always greatly increased the rate of decomposition to zinc metal at room temperature. After this trend had been noticed, all solid products were filtered as quickly as possible. When Li_2ZnH_4 was prepared from $\text{Li}_2\text{Zn}(\text{CH}_3)_4$, no zinc metal lines were observed when the compound was stirred in the reaction mixture for only 1 hr before filtration.

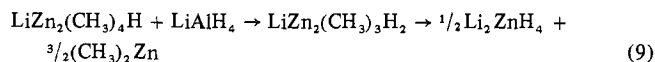
The route by which Li_2ZnH_4 is formed from $\text{LiZn}(\text{sec-}$

$C_4H_9)_3H$, $LiZn(CH_3)_2H$, and $LiZn_2(CH_3)_4H$ is not clear, especially in the case of $LiZn_2(CH_3)_4H$. A reasonable explanation for the formation of Li_2ZnH_4 from $LiZn(sec-C_4H_9)_2H$ or $LiZn(CH_3)_2H$ is that $LiAlH_4$ undergoes hydrogen-alkyl group exchange with the $LiZnR_2H$ compound in a stepwise fashion. After the first alkyl exchange step, it is suggested that $LiZnRH_2$ (where $R = CH_3$ or $sec-C_4H_9$) forms which could then disproportionate to Li_2ZnH_4 and ZnR_2 faster than it reacts with $LiAlRH_3$ (eq 8).



This explanation is supported by elemental analysis of the reaction mixtures from reduction of $LiZn(sec-C_4H_9)_2H$ and $LiZn(CH_3)_2H$ with $LiAlH_4$. The solid product from the reaction of $LiZn(sec-C_4H_9)_2H$ with $LiAlH_4$ had a molar ratio of $Li:Zn:H$ of 2:1:4. The filtrate contained one-half of the initial amount of zinc. Thus, the solid (Li_2ZnH_4) contained the other half. This is consistent with the disproportionation of an intermediate complex to equimolar amounts of di-*sec*-butylzinc and Li_2ZnH_4 . Evidently, di-*sec*-butylzinc was not reduced to zinc hydride by the intermediate aluminum hydride species, $LiAl(sec-C_4H_9)_3$. The solid from the reaction of $LiZn(CH_3)_2H$ with $LiAlH_4$ had a molar ratio of $Li:Zn:H$ of 1:1:3. The filtrate contained very little of the starting zinc compound and the X-ray powder diffraction pattern showed only lines for Li_2ZnH_4 and zinc metal. Thus, the solid product must be a mixture of Li_2ZnH_4 and ZnH_2 , where the ZnH_2 comes from reduction of $(CH_3)_2Zn$ with $LiAl(CH_3)_3$. A situation similar to this was encountered by Coates¹⁸ in the preparation of $LiBeH_3$. The X-ray powder diffraction pattern of the compound contained lines due to Li_2BeH_4 only, but the analysis showed a molar ratio of $Li:Be:H$ of 1:1:3. Coates concluded that the product was an equimolar mixture of Li_2BeH_4 and BeH_2 .

The mechanism of formation of Li_2ZnH_4 by reaction of $LiZn_2(CH_3)_4H$ with $LiAlH_4$ is not as well understood. Even less understandable is the reason why $LiZn_2(CH_3)_4H$ reacts so slowly with $LiAlH_4$. It took 5 days for essentially all the zinc to appear in the solid whereas most of the "ate" complexes used in this work react with $LiAlH_4$ instantaneously to yield solid products containing all of the original zinc. The solid did contain $Li:Zn$ in a ratio of 1:2, but the active hydrogen was very low indicating considerable decomposition. It is possible that the initial reduction product was $LiZn_2H_5$, which decomposed to Li_2ZnH_4 and ZnH_2 . A more reasonable reaction path consists of a slow stepwise exchange of a methyl group of $LiZn_2(CH_3)_4H$ to the intermediate complex, $LiZn_2(CH_3)_3H_2$, which could then disproportionate to Li_2ZnH_4 and $(CH_3)_2Zn$ according to eq 9.



The $(CH_3)_2Zn$ would then presumably be reduced rapidly in the presence of $LiAlH_4$ to ZnH_2 . The major part of the decomposition is probably due to decomposition of ZnH_2 .

The vacuum dta-tga of Li_2ZnH_4 is shown in Figure 2. Li_2ZnH_4 decomposes evolving noncondensable gases at 136 and 310°. The thermal effect for the first gas evolution contains a sharp exotherm superimposed on a broad deep endotherm. The thermal effect for the next gas evolution is a small endotherm. The ratio of weight loss for the two gas evolutions is 1:1. The first gas evolution is attributed to decomposition of Li_2ZnH_4 to LiH and ZnH_2 with simul-

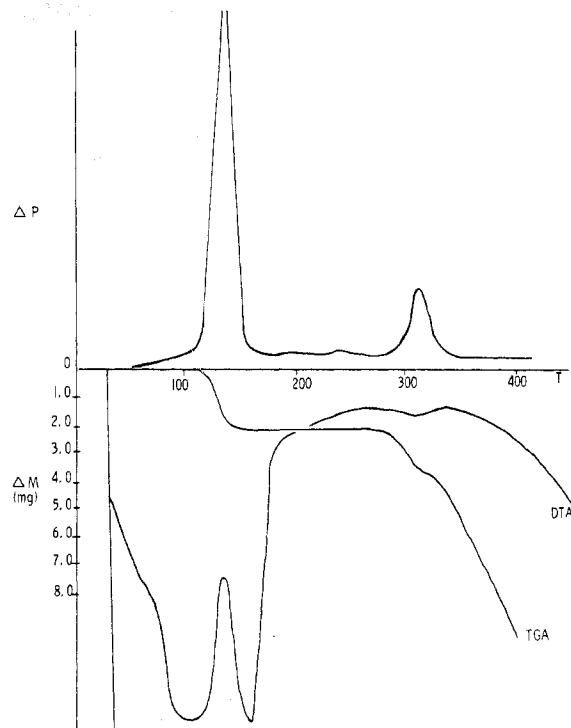
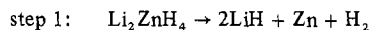
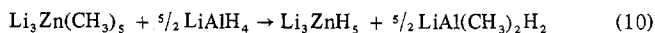


Figure 2. Vacuum dta-tga of Li_2ZnH_4 .

taneous decomposition of ZnH_2 . The last endotherm is due to the decomposition of LiH . An X-ray powder diffraction pattern taken after the first step showed the presence of LiH and Zn metal. The steps involved in the decomposition are shown below.



Li_3ZnH_5 . In their low-temperature nmr work on the system $CH_3Li-(CH_3)_2Zn$, Seitz and Brown¹⁶ reported the existence of two complexes, $Li_2Zn(CH_3)_4$ and $Li_3Zn(CH_3)_5$. Since reduction of $Li_2Zn(CH_3)_4$ with $LiAlH_4$ yields Li_2ZnH_4 , reduction of $Li_3Zn(CH_3)_5$ with $LiAlH_4$ should provide a convenient route to Li_3ZnH_5 (eq 10).

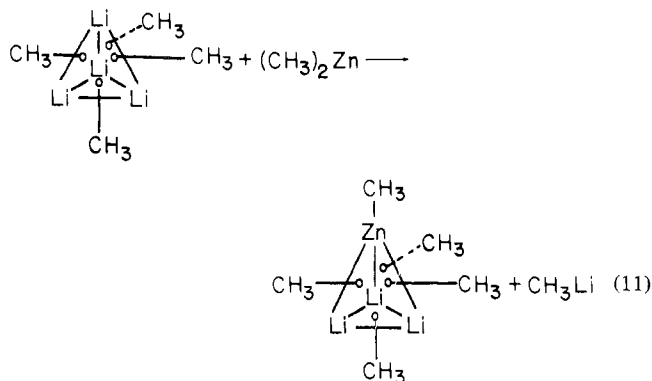


The reaction of $Li_3Zn(CH_3)_5$ with $LiAlH_4$ in diethyl ether at room temperature gave Li_3ZnH_5 in 100% yield. The product contained a small amount of $LiAlH_4$ which precipitated with the product. The X-ray powder diffraction pattern (Table I) did not contain any lines due to Li_2ZnH_4 , ZnH_2 , or LiH ; therefore, the product of the reaction is not a physical mixture. The infrared spectrum contained two strong and two moderate bands. The two strong bands are centered at 680 and 1550 cm^{-1} . The two moderate bands are centered at 990 and 1280 cm^{-1} . Although the structure of Li_3ZnH_5 might be similar to that proposed by Brown¹⁶ for $Li_3Zn(CH_3)_5$, because of the insolubility of the hydride, molecular association, ir, and nmr data could not be obtained to establish this point.

The vacuum dta-tga of this compound, run several months after it was originally prepared, was similar to that observed for Li_2ZnH_4 . At this point it was thought that Li_3ZnH_5 decomposed slowly over a period of months to Li_2ZnH_4 and LiH ; however, subsequent attempts to reprepare Li_3ZnH_5 have failed. In each case the product was a mixture of Li_2ZnH_4 and LiH . This is the only complex metal hydride reported in this work, the preparation of which could not

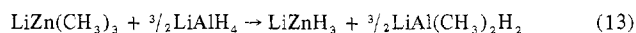
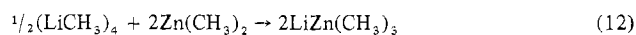
be reproduced. In spite of this result, the original data indicated the unequivocal formation of Li_3ZnH_5 .

LiZnH_3 . $\text{Li}_3\text{Zn}(\text{CH}_3)_5$ has been reported¹⁶ to be formed in diethyl ether by substitution of one dimethylzinc molecule for one methyllithium unit in the methyllithium tetramer (eq 11). $\text{LiZn}(\text{CH}_3)_3$ could then be formed by substitution



of two methyllithium units in the methyllithium tetramer by two molecules of dimethylzinc. $\text{LiZn}(\text{CH}_3)_3$ formed in this way should provide an excellent precursor to LiZnH_3 .

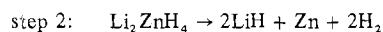
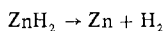
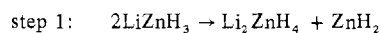
The reaction of a 1:1 mixture of methyllithium and dimethylzinc with LiAlH_4 in diethyl ether did produce LiZnH_3 (eq 12 and 13). The X-ray powder diffraction pattern of



LiZnH_3 (Table I) was very different from that of Li_2ZnH_4 or Li_3ZnH_5 and did not contain any lines in common with LiH or ZnH_2 . Little information concerning the structure of LiZnH_3 is available since the compound is not soluble enough to obtain molecular association and nmr data.

The vacuum dta-tga of LiZnH_3 is shown in Figure 3. It contained noncondensable gas evolutions at 97, 136, and 290°. The gas evolution at 97° was accompanied by a strong exothermal effect and is probably due to disproportionation of LiZnH_3 to Li_2ZnH_4 and ZnH_2 , with simultaneous decomposition of ZnH_2 . The decomposition of ZnH_2 normally occurs between 90 and 100°. The fact that the next two gas evolutions correspond to those accompanying decomposition of Li_2ZnH_4 supports this proposal.

The thermal decomposition of LiZnH_3 is believed to occur in essentially three steps.



The first step is slow compared to the second which shows ZnH_2 decomposing very rapidly once formed. The decomposition of Li_2ZnH_4 occurs at higher temperatures.

LiZn_2H_5 and LiZn_3H_6 . The 1:2 and 1:3 mixtures of methyllithium and dimethylzinc were allowed to react with LiAlH_4 in diethyl ether. The solid compounds obtained had Li:Zn:H ratios of 1:2:5 and 1:3:7. However, the X-ray powder diffraction patterns of the solids (Table I) contained lines due only to LiZnH_3 . Thus, the solid compounds are 1:1 and 1:2 mixtures of LiZnH_3 and ZnH_2 .

$\text{KZn}(\text{CH}_3)_2\text{H}$ and $\text{KZn}_2(\text{CH}_3)_4\text{H}$. In contrast to the reaction of di-*sec*-butylzinc with KH which yields K_2ZnH_4 directly, KH and dimethylzinc react in 1:1 ratio in either diethyl ether or tetrahydrofuran to form $\text{KZn}(\text{CH}_3)_2\text{H}$ in

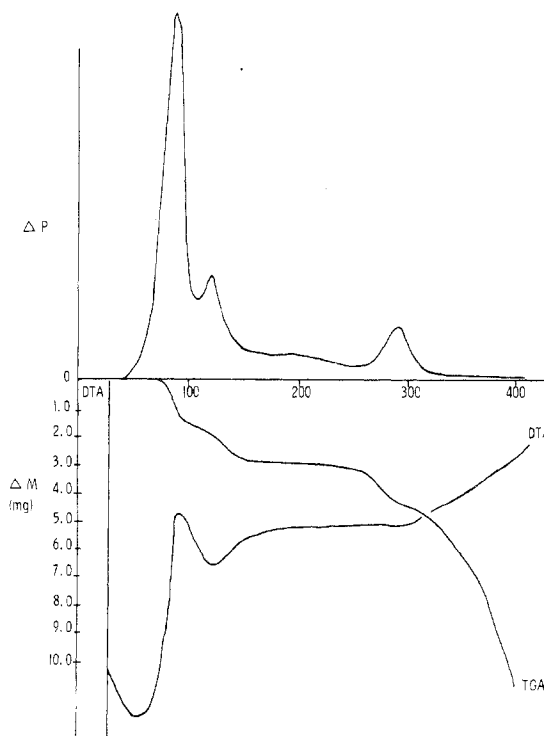
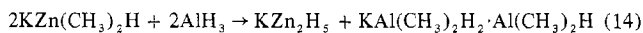


Figure 3. Vacuum dta-tga of LiZnH_3 .

quantitative yield. This complex had not been prepared previously; however, its properties were found to be analogous to those of $\text{LiZn}(\text{CH}_3)_2\text{H}$ and $\text{NaZn}(\text{CH}_3)_2\text{H}$ which had been prepared earlier by Shriver.⁹ Like the lithium and sodium complexes, $\text{KZn}(\text{CH}_3)_2\text{H}$ was insoluble in diethyl ether but soluble in tetrahydrofuran. Reaction of $\text{KZn}(\text{CH}_3)_2\text{H}$ was found to take place with another molecule of $(\text{CH}_3)_2\text{Zn}$ to give $\text{KZn}_2(\text{CH}_3)_4\text{H}$, which like the lithium and sodium complexes decomposed to $\text{KZn}(\text{CH}_3)_2\text{H}$ and $(\text{CH}_3)_2\text{Zn}$ when an attempt was made to isolate it as a solid.

KZn_2H_5 . The reaction of $\text{KZn}(\text{CH}_3)_2\text{H}$ with AlH_3 in tetrahydrofuran (AlH_3 was chosen as reducing agent because of the possibility of alkali metal exchange if LiAlH_4 were used) was selected as a convenient route to KZn_2H_5 . However, the reaction readily proceeds to give KZn_2H_5 (eq 14)



in quantitative yield. The X-ray powder diffraction pattern for KZn_2H_5 (Table II) contains no lines due to KH , ZnH_2 , or K_2ZnH_4 . The infrared spectrum of the filtrate containing the $\text{KAl}(\text{CH}_3)_2\text{H}_2 \cdot \text{Al}(\text{CH}_3)_2\text{H}$ showed a broad band in the Al-H stretching region centered at 1618 cm^{-1} . Me_2AlH absorbs at 1750 cm^{-1} in THF; thus, the species is not a mixture of $\text{Al}(\text{CH}_3)_2\text{H}$ and $\text{KAl}(\text{CH}_3)_2\text{H}_2$ in solution.

KZn_2H_5 was also formed by reduction of $\text{KZn}_2(\text{CH}_3)_4\text{H}$ with AlH_3 in tetrahydrofuran (eq 15). In this reaction very little potassium was found in the filtrate. The X-ray powder diffraction pattern of KZn_2H_5 obtained from this reaction is shown in Table II.

The vacuum dta-tga of KZn_2H_5 is shown in Figure 4. Large noncondensable gas evolutions occurred at 125, 223, and 267°. The ratio of the weight loss during the first gas evolution to that during the second was 3:1. The thermal effect for the first gas evolution showed a sharp endotherm superimposed on a broad exotherm. The exotherm is be-

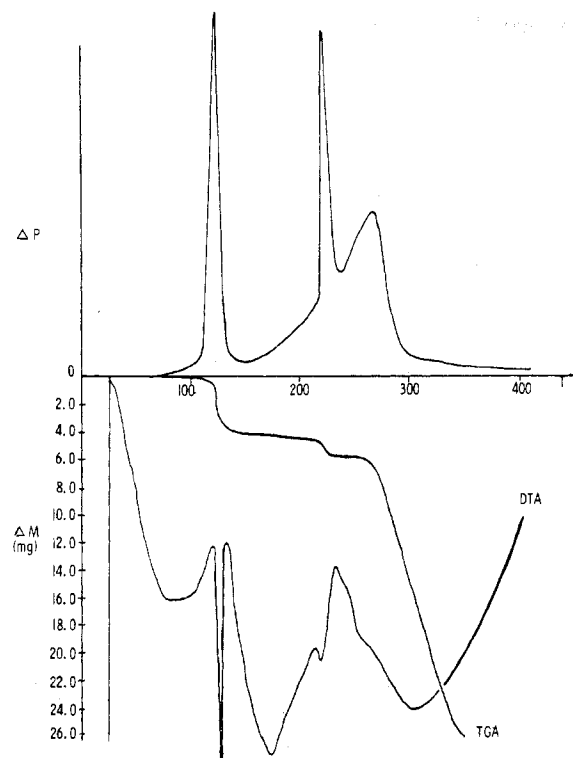
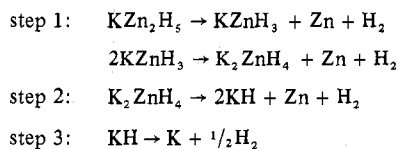


Figure 4. Vacuum dta-tga of KZn_2H_5 .

lieved to be due to decomposition of KZn_2H_5 to $KZnH_3$ and ZnH_2 with simultaneous decomposition of ZnH_2 to Zn and H_2 . The endotherm is believed to be due to disproportionation of $KZnH_3$ to K_2ZnH_4 and ZnH_2 with simultaneous decomposition of the ZnH_2 . The thermal effects for the second and third gas evolutions were endothermic. The second gas evolution is due to the decomposition of K_2ZnH_4 to KH and ZnH_2 with simultaneous decomposition of ZnH_2 . The third gas evolution is due to decomposition of KH . The mechanism of decomposition, shown in the three steps below, is supported by X-ray powder diffraction data, taken after the first two stages of gas evolution. The X-ray powder pattern taken after the first step showed lines for K_2ZnH_4 and Zn metal only. The X-ray powder pattern taken after the second step showed lines for KH and Zn metal. More evidence is provided by the fact that the ratio of the weight loss in step 1 to that in step 2 should be 3, which is what was found.



In order to substantiate that steps 2 and 3 are the only steps involved in the decomposition of K_2ZnH_4 , the dta-tga of K_2ZnH_4 was investigated. The vacuum dta-tga shown in Figure 5 contained one very broad peak at 285° with shoulders at 200 and 237° indicative of the evolution of a noncondensable gas. Further information concerning the decomposition of K_2ZnH_4 by observing the dta-tga under argon flush is shown in Figure 6. The dta-tga contained three well-separated weight losses with corresponding endotherms at 150 , 266 , and 355° . This differs somewhat from the dta-tga for K_2ZnH_4 obtained, under argon, in our earlier report.⁸ In the earlier work, K_2ZnH_4 was reported to have lost all solvent before 80° and have endothermal de-

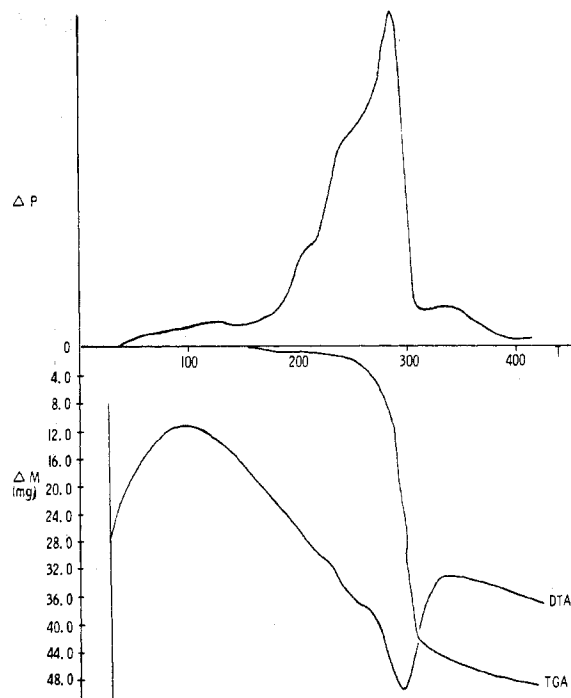


Figure 5. Vacuum dta-tga of K_2ZnH_4 .

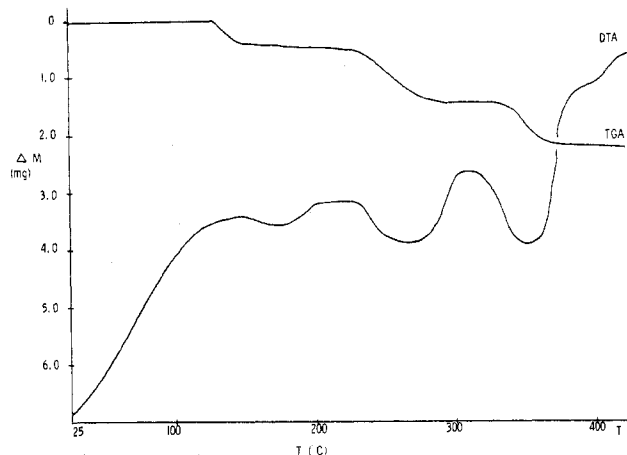


Figure 6. Dta-tga of K_2ZnH_4 under Ar.

composition steps at 242 , 292 , and 336° . No attempt was made to study the precise reactions involved in the decomposition steps. In the present work, the endothermal weight loss at 150° was found to be due to loss of solvent, since an X-ray powder diffraction pattern of a sample heated to 200° contained lines due only to K_2ZnH_4 . The endothermal weight loss at 266° can be represented by the reaction shown in eq 16 since an X-ray powder pattern of a sample heated



to 300° showed lines due only to KH and zinc metal. Thus, the last endotherm can be represented by the reaction shown in eq 17.



KZn_3H_7 . Reaction of a 1:3 mixture of KH and $(CH_3)_2Zn$ with AlH_3 in tetrahydrofuran gave a white solid with K:Zn:H ratio of 1:3:7; however, the X-ray powder diffraction pattern showed only lines for KZn_2H_5 . Thus, the compound must be a 1:1 mixture of KZn_2H_5 and ZnH_2 .

$KZnH_3$. The reaction of $KZn(CH_3)_2H$ with $LiAlH_4$ in

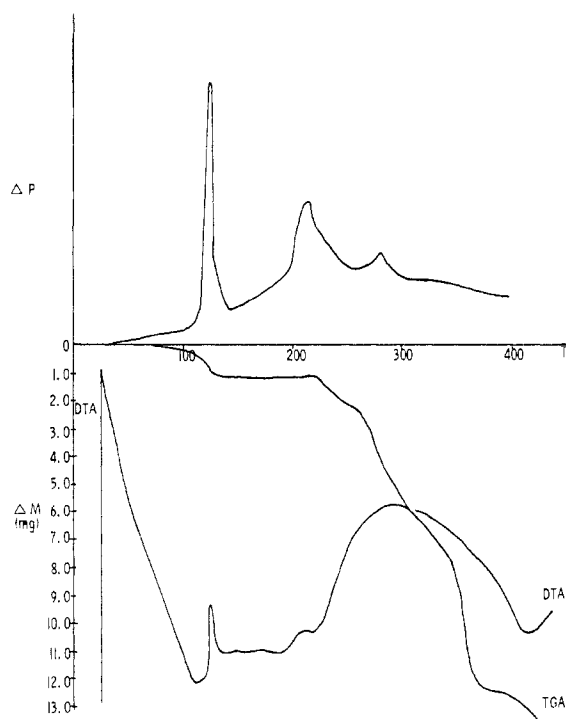
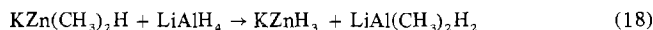


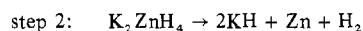
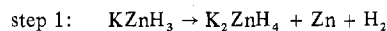
Figure 7. Vacuum dta-tga of KZnH_3 .

tetrahydrofuran gave KZnH_3 (no alkali metal exchange) in quantitative yield (eq 18). The X-ray powder diffraction

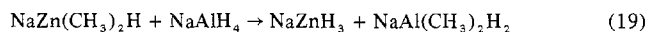


pattern of KZnH_3 (Table II) did not contain any lines due to KZn_2H_5 , K_2ZnH_4 , ZnH_2 , or KH .

The vacuum dta-tga of KZnH_3 is shown in Figure 7. Three stages of noncondensable gas evolution were observed at 125, 213, and 280°. The weight losses accompanying the first and second stages of gas evolution were equivalent. The X-ray powder diffraction pattern of the solid left after the first gas evolution showed lines for K_2ZnH_4 and Zn only. The X-ray powder pattern of the solid left after the second gas evolution showed lines due to KH and Zn . These data lead to the following suggested decomposition pattern of KZnH_3 . The weight losses during steps 1 and 2 should be equivalent. This is what was observed.



NaZnH_3 . The reaction of $\text{NaZn}(\text{CH}_3)_2\text{H}$ with NaAlH_4 in tetrahydrofuran gave NaZnH_3 (eq 19). The X-ray diffrac-



tion pattern (Table III) was identical with that reported by Shriver¹⁰ in his preparation of NaZnH_3 . [Shriver's preparation involved thermal decomposition of $\text{NaZn}_2(\text{CH}_3)_2\text{H}_3$ under vacuum to give NaZnH_3 and $(\text{CH}_3)_2\text{Zn}$]. Vacuum dta-tga analysis of NaZnH_3 , shown in Figure 8, showed a strong exotherm at 72° and moderate endotherms at 104, 183, and 250°. The simultaneous weight loss curve showed inflections that correspond to equivalent weight losses at each of the endotherms and no weight loss at the exotherm. The first endotherm (104°) corresponds to the thermal decomposition of ZnH_2 ; therefore, the exotherm at 72° can be attributed to disproportionation of NaZnH_3 to Na_2ZnH_4 and ZnH_2 . This observation explains why NaZnH_3 turns

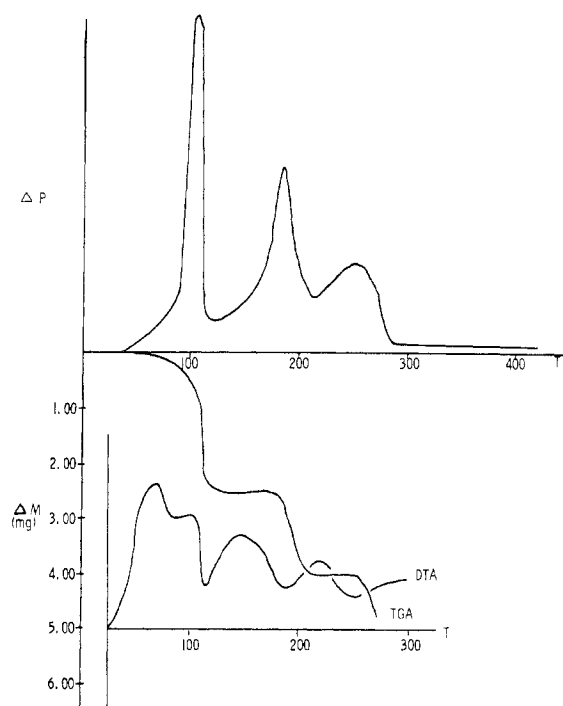


Figure 8. Vacuum dta-tga of NaZnH_3 .

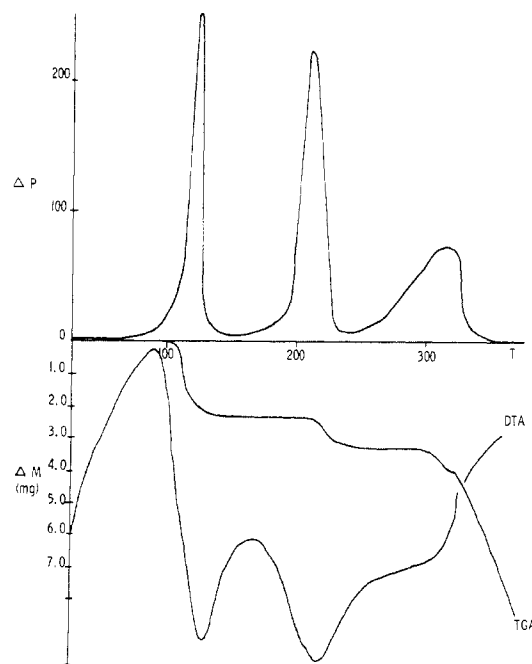
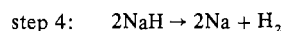
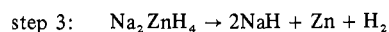
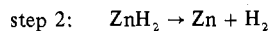
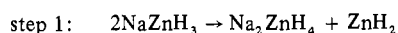


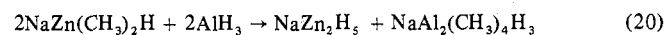
Figure 9. Vacuum dta-tga of Na_2ZnH_5 .

black on standing at room temperature (a phenomenon reported by Shriver⁹ and observed by the authors). The endotherm at 183° corresponds to the decomposition of Na_2ZnH_4 and the endotherm at 250° corresponds to the decomposition of NaH . The dta-tga reported previously by us is different from the one reported here; however, the difference is probably due to the fact that the earlier dta-tga was run under argon at 1 atm of pressure, whereas the dta-tga reported here was carried out under vacuum. Thermal decomposition of NaZnH_3 is believed to proceed by the following series of steps.



The reaction of $\text{NaZn}_2(\text{CH}_3)_4\text{H}$ with NaAlH_4 also yielded NaZnH_3 . The X-ray powder diffraction pattern of NaZnH_3 prepared by this route is given in Table III. The mechanism by which NaZnH_3 was formed in this reaction is not understood at present.

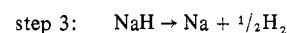
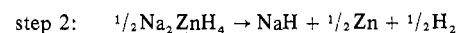
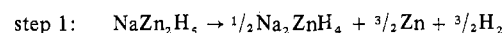
NaZn_2H_5 . In a manner similar to the reaction of $\text{KZn}(\text{CH}_3)_2\text{H}$ with AlH_3 which formed KZn_2H_5 , AlH_3 was also found to react with $\text{NaZn}(\text{CH}_3)_2\text{H}$ to form NaZn_2H_5 (eq 20). The X-ray powder pattern of NaZn_2H_5 (Table III)



contained no lines due to NaH , ZnH_2 , Na_2ZnH_4 , or NaZnH_3 . The infrared spectrum of the filtrate remaining after filtration of the solid NaZn_2H_5 showed a very broad band in the Al-H stretching region centered at 1610 cm^{-1} . In view of this spectrum and elemental analysis of the filtrate, the product in solution is believed to be a complex between Me_2AlH and $\text{NaAlMe}_2\text{H}_2$.

The vacuum dta-tga of NaZn_2H_5 is shown in Figure 9. Large evolutions of noncondensable gas occurred at 123, 210, and 315° . The ratio of the weight loss during the first gas evolution to that during the second and third ones was 3:1:1. The thermal effect for the first gas evolution was endothermic. This endotherm is believed to be due to dis-

proportionation of NaZn_2H_5 to Na_2ZnH_4 and ZnH_2 with simultaneous decomposition of the ZnH_2 . The thermal effects for the second and third gas evolutions were also endothermic. The second gas evolution is due to decomposition of Na_2ZnH_4 to NaH and ZnH_2 with simultaneous decomposition of ZnH_2 . The third gas evolution is due to decomposition of NaH . The mechanism of decomposition, shown in the three steps below, is supported by X-ray powder diffraction data, taken after the first two stages of gas evolution. The X-ray powder pattern taken after the first step showed lines for Na_2ZnH_4 and Zn metal only. The X-ray powder pattern taken after the second step showed lines for NaH and Zn metal. More evidence is provided by the fact that the ratio of the weight losses in the three steps should be 3:1:1, which is what was observed.



Acknowledgment. We are indebted to the Office of Naval Research (Contract No. N000 14-67-A-0159-0005 and Contract Authority No. NR-93-050/12-5-67-429) for support of this work.

Registry No. LiH , 7580-67-8; (*sec*- C_4H_9) $_2\text{Zn}$, 7446-94-8; LiAlH_4 , 16853-85-3; Li_2ZnH_4 , 38829-84-4; $(\text{CH}_3)_2\text{Zn}$, 544-97-8; CH_3Li , 917-54-4; LiZnH_3 , 38829-83-3; Li_3ZnH_5 , 38887-62-6; KH , 7693-26-7; $\text{KZn}(\text{CH}_3)_2\text{H}$, 41202-98-6; AlH_3 , 7784-21-6; KZn_2H_5 , 37276-96-3; NaH , 7646-69-7; NaAlH_4 , 13770-96-2; NaZnH_3 , 34397-46-1; NaZn_2H_5 , 39356-34-8.

Contribution from the Department of Chemistry, State University of New York at Buffalo, Buffalo, New York 14214

Syntheses and Properties of Unsymmetrical Boron-Disubstituted Borazine Derivatives

O. T. BEACHLEY, Jr.

Received February 20, 1973

A series of unsymmetrical B-disubstituted borazine derivatives, $\text{H}(\text{Cl})(\text{OCN})\text{B}_3\text{N}_3\text{H}_3$, $\text{H}(\text{Cl})(\text{CN})\text{B}_3\text{N}_3\text{H}_3$, $\text{H}(\text{CN})(\text{OCN})\text{B}_3\text{N}_3\text{H}_3$, $\text{H}(\text{OCN})_2\text{B}_3\text{N}_3\text{H}_3$, and $\text{H}(\text{CN})_2\text{B}_3\text{N}_3\text{H}_3$, has been prepared and characterized. The synthetic reactions and the nature of the resulting compounds have been investigated in order to more fully elucidate the effects of substituents on the chemical and physical properties of the borazine ring. The substituents in these new compounds represent unique combinations of electron-withdrawing and electron-donating groups. These B-disubstituted borazine compounds were synthesized from an appropriate B-chloroborazine and silver(I) salt by reaction at only a B-Cl bond. The compounds could not be prepared from the B-monosubstituted borazine by reaction with a silver(I) salt. A hydrogen bound to boron in the B-disubstituted borazine was unreactive to silver(I) salts for the conditions used in our experiments. Our previous work has shown that $\text{H}_3\text{B}_3\text{N}_3\text{H}_3$ readily reacts with silver(I) salts. Therefore, our new reactivity data represent the first clear example of a substituent effect in borazine chemistry. The ^1H nmr data for the B-disubstituted borazine derivatives indicate that there is an additivity relationship for the effects of substituents on the chemical shift of the NH protons. However, the additivity relationship is only observed for those substituents for which the ortho and para NH protons are magnetically equivalent in the B-monosubstituted derivative.

One of the most intriguing problems in synthetic inorganic chemistry involves the preparation of unsymmetrically substituted borazine derivatives. Significant advancements have been made in the syntheses of B-monosubstituted borazines. There are many reactions which can be used to prepare only specific B-monosubstituted compounds.^{1,2} However, there are no routes designed for the B-disubstituted compounds. All of the simple B-disubstituted borazine

derivatives have been previously obtained as products from reactions designed to prepare B-monosubstituted compounds²⁻⁴ or from disproportionation reactions² of monosubstituted compounds. Therefore, a knowledge of synthetic reactions for B-disubstituted borazine derivatives would be significant and could provide interesting data on the nature of substituent effects. Previous experiments have demon-

(1) O. T. Beachley, Jr., *J. Amer. Chem. Soc.*, **93**, 5066 (1971).
 (2) O. T. Beachley, Jr., *J. Amer. Chem. Soc.*, **92**, 5372 (1970).

(3) O. T. Beachley, Jr., *Inorg. Chem.*, **8**, 2665 (1969).
 (4) R. Maruca, O. T. Beachley, Jr., and A. W. Laubengayer, *Inorg. Chem.*, **6**, 575 (1967).